Study of time dependent free convective kerosene-nanofluid flow with viscous dissipation past a porous plate

Cite as: AIP Conference Proceedings **2246**, 020009 (2020); https://doi.org/10.1063/5.0014451
Published Online: 28 July 2020

M. P. Mallesh, V. Rajesh, M. Kavitha, et al.

Study of Time Dependent Free Convective Kerosene-Nanofluid Flow with Viscous Dissipation Past a Porous Plate

M.P.Mallesh[1,a)], V.Rajesh[2,b)] , M.Kavitha[3,c)], and Ali J. Chamkha[4,d)]

1Department of Mathematics, Koneru Lakshmaiah Education Foundation, Hyderabad Campus, Aziznagar Village, Moinabad (M), R R Dist, Telangana, India.
2 Department of Mathematics, GITAM (Deemed to be University), Hyderabad Campus, Rudraram Village, Patancheru (M), Medak, Telangana, India.
3 Department of Mathematics, Global Institute of Engineering and Technology, Chilkur Village, Moinabad(M), R R Dist, Telangana, India.
4 Mechanical Engineering Department, Prince Mohammad Endowment for Nanoscience and Technology, Prince Mohammad Bin Fahd University, Al-Khobar 31952, Saudi Arabia.

a)E-mail address: malleshmardanpally@gmail.com
b)E-mail address: v.rajesh.30@gmail.com
c)E-mail address: kavitha.itikala@gmail.com
d)E-mail address: achamkha@pmu.edu.sa

Abstract. In this article, we perceived the amplification of heat transfer of viscous incompressible kerosene oil based nanofluid past a porous plate accompanied by viscous dissipation. A robust Galerkin type numerical finite element technique is adopted to solve the equations which model the flow. The alterations in velocity and temperature for diverse values of appropriate parameters such as suction parameter (λ), Eckert Number (E), volume fraction (δ), thermal Grashof number (G) are examined in the form of graphs and for skin friction coefficient as well as Nusselt number in the form of tables. This study contributes to enhance the cooling/heating performance of industrial and engineering systems.

Keywords: Free convection, kerosene-nanofluid, vertical porous plate, Galerkin finite element method, viscous dissipation, partial differential equations.

INTRODUCTION

A notable provocative interdisciplinary area of research is to improve the cooling/heating performance, life span and capabilities of engineering and industrial systems. Instantaneous usage of these industrial equipment's leads to the release of hot gases as a consequence, they experience high temperature which leads to the damage of the equipment. To safeguard the walls of these equipment's they made to be cooled, numerous ways of cooling strategies are implemented to safeguard them. The vital factors which control the cooling achievement of the walls of engineering and industrial systems are fluid thermo-physical properties and flow velocity. Kerosene has special features such as high cooling capabilities and greater heat-absorbing capacity at above its critical values of temperature and pressure. Due to these reasons it is used as one of the fuels, like, China No:3 kerosene, n-decane and JP-7 [1-4]. Mostafa Mahmoodi and Sh.Kandelousi [5] examined analytically the cooling phenomena of liquid

International Conference on Mathematical Sciences and Applications (ICMSA-2019)
AIP Conf. Proc. 2246, 020009-1–020009-9; https://doi.org/10.1063/5.0014451
Published by AIP Publishing. 978-0-7354-2005-2/$30.00

rocket engine. In this scientific era of smart age the smart fluid known as nano fluid primarily tagged by Choi[6]. Nanofluids are made by dispersing ultra fine nonmetered sized particles (diameter less than 100nm) like Al, Cu, Si, Ag and Ti or their oxides diffused in a pure fluid like water, ethylene, glycol, toluene and oil. They have improved favorable thermo-physical properties, for example thermal conductivity, lower specific heat, and enhanced heat transfer coefficients in comparison with conventional fluids. Nanofluids have several cooling applications which includes cooling of nuclear reactors, automobile engines, electric transformers, silicon mirrors, electronic equipment's, heat exchangers, welding equipment's and micro-electro-mechanical system.

In engineering and industrial systems free convective flow and heat transfer on vertical geometries have several important functions for instance solar-collectors, electrical and microelectronic equipment's, petroleum reservoirs, geothermal engineering, thermal buildings insulation, etc. Buoyancy-driven flows arise due to the variation in temperature as a result density changes consequently buoyancy forces acts upon the fluid elements. To discuss the prominence of buoyancy force on heat transfer due to fluid flow under several physical conditions, numerous investigations have taken place. Aziz and Khan [7] examined the phenomena of buoyant flow of a nanofluid above an upright plate. Kuznetsov and Nield [8] examined the analytical solution of buoyant flow of a nanofluid above an erect plate. Turkyilmazoglu [9] studied the features of time dependent flows and heat transfer of some nanofluids above a stimulating plate. Rajesh et al [10] developed transient numerical modeling of buoyant flow of a nanofluid with variable temperature over an upright plate. Nilankush Acharya et al [11] surveyed the compressive flow of Water-Cu and kerosene-Cu nanofluids between two parallel plates. Recently, several experimental studies [12-14] on kerosene based nanofluids are carried out. The buoyancy driven flow of a Water-Al_2O_3 nanofluid was developed by Congedo et al [15]. A numerical model for time dependent buoyant flow of a nanofluid above an erect plate was developed by Rajesh et al [16]. The irreversible phenomena in which the fluid does a work on adjacent layers with the help of shear forces is transmuted into heat is known as viscous dissipation. In this process mechanical energy is transmuted into heat energy. Viscous dissipation effects plays a vital role in geophysical flows and aerodynamics. Time dependent 2D flow of hydromagnetic fluid with heat and mass transfer accompanied by fluctuating viscosity and viscous dissipation within a porous medium above a stimulating erect plate was inspected by Singh [17]. Time dependent flow of micropolar fluid with heat transfer accompanied by viscous dissipation was discussed by Kishan and Deepa [18]. Rajesh et al [19] analyzed the impact of viscous dissipation accompanied by hydromagnetic nanofluid flow over an upright porous plate.

The chief aim of this research article is to explore the problem of time dependent laminar free convective 2D boundary layer flow of a viscous, incompressible kerosene-nanofluid and heat transfer above a stimulating porous plate owing to viscous dissipation. The nonlinear coupled dimensionless partial differential equations which control the fluid flow along with conditions are elucidated by employing a robust Galerkin finite element procedure. The alterations in the velocity and temperature for diverse values of appropriate parameters such as parameter λ, E, δ, G are examined in the form of graphs and for C_f as well as Nu in the form of tables. The current study contributes to enhance the cooling/heating performance of industrial and engineering systems.

MATHEMATICAL FORMULATION

In this article we assume Cartesian coordinate system $\left(\mathrm{x}^*, y^*\right)$ such that x^*-axis is aligned vertically upwards in the direction of the plate, while the traverse coordinate (y^*-axis) is anchored normal to the plate. In the beginning, both the plate and fluid are kept static and retained at free stream temperature θ_∞^* for all $t' \le 0$. Subsequently at time $t' > 0$, the plate commence to be in motion with invariable velocity $u_{1_0}^*$. The temperature of the plate is elevated to $\theta^* = \theta_w^*$ and is maintained at the same level. In the present context we assume single phase nanofluids accompanied by local thermal equilibrium between the nanoparticles and base fluids to avoid the slip between them. Since the length of the plate is infinite, the velocity and temperature portraitures are functions of y^* and t^* only. The fluid comprises of Cu, Co, Ag, TiO_2, Al_2O_3 as nanoparticles with kerosene as a base fluid. Thermal and physical properties of the nanoparticles and kerosene (Uddin et al [20]) are depicted in Table 1.

We adopt Tiwari and Das [21] nanofluid model and Boussinesq approximation (Schlichting and Gersten, [22]) in this flow, with these presumptions the equations that controls the physical phenomena are here under:

$$\frac{\partial u_2^*}{\partial y^*} = 0 \tag{1}$$

$$\frac{\partial u_1^*}{\partial t^*} + u_2^* \frac{\partial u_1^*}{\partial y^*} = \nu_{nf} \frac{\partial^2 u_1^*}{\partial y^{*2}} + \frac{(\rho\beta)_{nf}}{\rho_{nf}} g\left(\theta^* - \theta_\infty^*\right) \tag{2}$$

$$\frac{\partial \theta^*}{\partial t^*} + u_2^* \frac{\partial \theta^*}{\partial y^*} = \frac{\kappa_{nf}}{\left(\rho C_p\right)_{nf}} \frac{\partial^2 \theta^*}{\partial y^{*2}} + \frac{\mu_{nf}}{\left(\rho C_p\right)_{nf}} \left(\frac{\partial u_1^*}{\partial y^*}\right)^2 \tag{3}$$

The conditions are given below:

$$t^* \le 0: \; u_1^* = 0, \quad \theta^* = \theta_\infty^* \quad \text{for all} \quad y^*$$

$$t^* > 0: \; u_1^* = u_{1_0}^*, \quad \theta^* = \theta_w^* \quad \text{for all} \quad y^* = 0$$

$$u_1^* \to 0, \quad \theta^* \to \theta_\infty^* \quad \text{as} \quad y^* \to \infty \tag{4}$$

Equation (1) gives

$$u_2^* = -u_{2_0}^* \left(u_{2_0}^* > 0\right) \tag{5}$$

Where $u_{2_0}^*$ is the constant suction velocity and the negative sign indicates that it is towards the plate.

Effective density $\rho_{nf} = \delta\rho_s + (1-\delta)\rho_f$

Thermal expansion coefficient $(\rho\beta)_{nf} = \delta(\rho\beta)_s + (1-\delta)(\rho\beta)_f$ (6)

Heat capacitance $(\rho C_p)_{nf} = \delta(\rho C_p)_s + (1-\delta)(\rho C_p)_f$

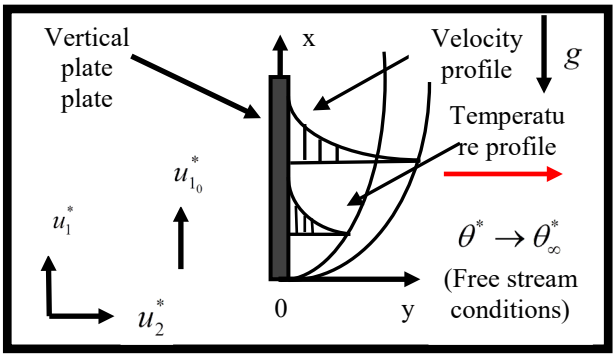

FIGURE 1: Physical geometry

The relevant thermal conductivity according to Maxwell-Garnett model [23] for nanofluids:

$$\frac{\kappa_{eff}}{\kappa_f} = \frac{\kappa_s + 2\kappa_f - 2\delta\left(\kappa_f - \kappa_s\right)}{\kappa_s + 2\kappa_f + \delta\left(\kappa_f - \kappa_s\right)} \tag{7}$$

The relevant dynamic viscosity according to Brinkman model[24] of the nanofluid is:

$$\mu_{nf} = \frac{\mu_f}{(1-\delta)^{2.5}} \tag{8}$$

The relevant dimensionless parameters are as:

$$u_1 = \frac{u_1^*}{u_{1_0}^*},\ t = \frac{t' u_{1_0}^*}{\nu_f},\ y = \frac{y^* u_{1_0}^*}{\nu_f} = \frac{y^*}{L_{ref}},\ \theta = \frac{\theta^* - \theta_\infty^*}{\theta_w^* - \theta_\infty^*}, G = \frac{g\beta_f \nu_f \left(\theta_w^* - \theta_\infty^*\right)}{\left(u_{1_0}^*\right)^3},\ P_r = \frac{\nu_f}{\alpha_f} = \frac{\left(\mu C_p\right)_f}{k_f},$$

$$\lambda = -\frac{u_2^*}{u_{1_0}^*},\ E = \frac{u_{1_0}^{*2}}{\left(C_p\right)_f \left(\theta_w^* - \theta_\infty^*\right)} \tag{9}$$

Table 1: Kerosene and nanoparticles thermo-physical properties

	Kerosene	Al_2O_3	Cu	TiO_2	Ag	Co
$\rho\left(Kg\,m^{-3}\right)$	780	3970	8933	4250	10500	8900
$C_p\left(J\,Kg^{-1}K^{-1}\right)$	2090	765	385	686.2	235	420
$\kappa\left(Wm^{-1}K^{-1}\right)$	0.149	40	401	8.9528	429	100
$\beta\times10^{-5}\left(K^{-1}\right)$	99	0.85	1.67	0.9	1.89	1.3

With the relevant dimensionless variables (9), Equations (2)-(3) become

$$\frac{\partial u_1}{\partial t} - \lambda \frac{\partial u_1}{\partial y} = \frac{1}{(1-\delta)^{2.5}} \frac{1}{\left(1-\delta+\delta\left(\frac{\rho_s}{\rho_f}\right)\right)} \frac{\partial^2 u_1}{\partial y^2} + \frac{\left(1-\delta+\delta\frac{(\rho\beta)_s}{(\rho\beta)_f}\right)}{\left(1-\delta+\delta\frac{(\rho)_s}{(\rho)_f}\right)} G\theta \tag{10}$$

$$\frac{\partial \theta}{\partial t} - \lambda \frac{\partial \theta}{\partial y} = \frac{k_{nf}}{k_f} \frac{1}{\left(1-\delta+\delta\frac{\left(\rho C_p\right)_s}{\left(\rho C_p\right)_f}\right)} \frac{1}{P_r} \frac{\partial^2 \theta}{\partial y^2} + \frac{1}{(1-\delta)^{2.5}} \frac{1}{\left(1-\delta+\delta\frac{\left(\rho C_p\right)_s}{\left(\rho C_p\right)_f}\right)} E\left(\frac{\partial u_1}{\partial y}\right)^2 \tag{11}$$

The relevant dimensionless conditions are:

$t \le 0:\ u_1 = 0, \quad \theta = 0 \quad \text{for all} \quad y$

$t > 0:\ u_1 = 1, \quad \theta = 1 \quad \text{at} \quad y$

$u_1 \to 0, \quad \theta \to 0 \quad \text{as} \quad y \to \infty$ (12)

Let $A_1 = \frac{1}{(1-\delta)^{2.5}} \frac{1}{\left(1-\delta+\delta\left(\frac{\rho_s}{\rho_f}\right)\right)}, \quad A_2 = \frac{\left(1-\delta+\delta\frac{(\rho\beta)_s}{(\rho\beta)_f}\right)}{\left(1-\delta+\delta\frac{(\rho)_s}{(\rho)_f}\right)},$

$$A_3 = \frac{k_{nf}}{k_f}\frac{1}{\left(1-\delta+\delta\dfrac{\left(\rho C_p\right)_s}{\left(\rho C_p\right)_f}\right)}, \quad A_4 = \frac{1}{\left(1-\delta\right)^{2.5}}\frac{1}{\left(1-\delta+\delta\dfrac{\left(\rho C_p\right)_s}{\left(\rho C_p\right)_f}\right)}.$$

Now the equations (10) and (11) in terms of $A_{1,}\ A_{2,}\ A_{3,}\ and\ A_4$ are

$$\frac{\partial u_1}{\partial t} - \lambda\frac{\partial u_1}{\partial y} = A_1\frac{\partial^2 u_1}{\partial y^2} + A_2 G\,\theta \tag{13}$$

$$\frac{\partial \theta}{\partial t} - \lambda\frac{\partial \theta}{\partial y} = A_3\frac{1}{P_r}\frac{\partial^2 \theta}{\partial y^2} + EA_4\left(\frac{\partial u_1}{\partial y}\right)^2 \tag{14}$$

The governing dimensionless equations (13) and (14) along with the relevant conditions (12) have been computed by employing a robust Galerkin type finite element technique.

ENGINEERING QUANTITIES

Most important physical quantities which are defined at the wall are C_f and Nu as mentioned below:

$$C_f = \frac{\tau_w}{\rho_f\, u_{1_0}^{*2}}, \quad Nu = \frac{q_w L_{ref}}{\kappa_f\left(\theta_w^* - \theta_\infty^*\right)} \tag{15}$$

Here τ_w is shear stress and q_w is heat flux (rate of heat transfer) as :

$$\tau_w = \mu_{nf}\left(\frac{\partial u_1^*}{\partial y^*}\right)_{y^*=0}, \quad q_w = -\kappa_{nf}\left(\frac{\partial \theta^*}{\partial y^*}\right)_{y^*=0} \tag{16}$$

With the help of dimensionless variables (9), we get
The dimensionless form of

$$C_f = \frac{1}{\left(1-\delta\right)^{2.5}}\left(\frac{\partial u_1}{\partial y}\right)_{y=0} \tag{17}$$

and the Nusselt number in dimensionless form

$$Nu = -\frac{\kappa_{nf}}{\kappa_f}\left(\frac{\partial \theta}{\partial y}\right)_{y=0} \tag{18}$$

Using the five-point approximation formula, the derivatives involved in Equations (17) and (18) are computed.

RESULT ANALYSIS

In this section we analyze simulated numerical solutions of pertinent controlling parameters namely G, E, δ, and t on C_f, Nu , velocity and temperature portraitures which are portrayed in the tabular and graphical form. Kerosene oil is tabbed as a conventional base fluid with *Cu*, *Ag*, TiO_2, Al_2O_3, *Co* nanoparticles. In the present

context we have taken spherical shaped nanoparticles with volume fraction in the range of $0 \le \delta \le 0.04$, and thermal conductivity, dynamic viscosity from equations (7) and (8) respectively. For base fluid $P_r = 21$ is fixed.

Figures 2 and 3 demonstrates the influence of controlling parameters λ, G, E, for temperature and velocity portraitures. From figure 2 the velocity of kerosene- Al_2O_3 nanofluid rises with rise in G which coincides physically, since G defines the proportion of buoyant force to viscous force. With rise in G the velocity grows inside the boundary layer this is due to the impact of thermal buoyancy. From Figure 3, we pointed that the temperature rises owing to enhancement in G. It is true palpably since the terms connected with G behaves as a strong source of heat in the momentum equation. Moreover, it is noted that from figures 2 and 3 the velocity and temperature decrease with rise in λ. Application of suction at the surface prompts the fluid into the surface and accordingly the momentum and thermal boundary-layers reduced with rise in λ. From figures 2 and 3 the velocity and temperature are found to grow with the growth in E. This is true since the E, is the proportion of kinetic energy to the enthalpy in the flow. It exemplifies the modification of kinetic energy into mechanical energy and this energy is released in the form of heat.

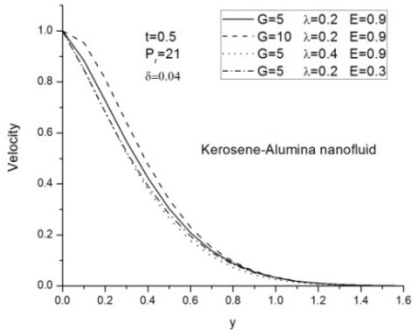

FIGURE 2: Velocity portraitures of G, E, λ

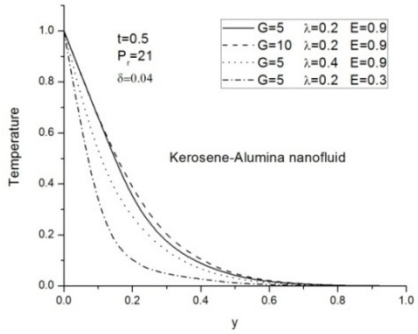

FIGURE 3:Temperature portraitures of G, E, λ

Figures 4 and 5 presents the velocity and temperature portraitures of kerosene -Al_2O_3 nanofluid for variety of δ, t. The velocity and temperature grow with rise in 't'. Further, the velocity and temperature of kerosene -Al_2O_3 nanofluid are less than that of pure kerosene ($\delta = 0$) for all values of time t. Figure 4 reveals that the velocity portraitures of the kerosene -Al_2O_3 nanofluid reduces with in the boundary-layer with the progress in δ. Physically it is true, since inclusion of the nanoparticles make the fluid more viscous thus the motion of the fluid slows down. From figure 5 we observe that the temperature portraitures of kerosene -Al_2O_3 nanofluid depreciates with rise in δ, as an outcome thermal boundary-layer thickness lessens.

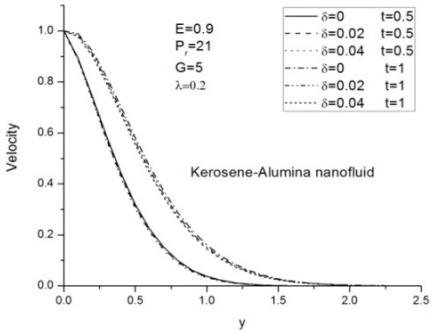

FIGURE 4: Velocity portraitures of δ, t

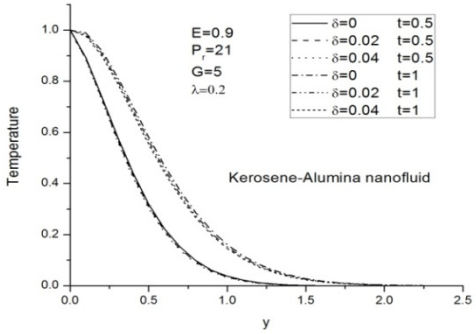

FIGURE 5: Temperature portraitures of δ, t

Table 2 exhibits the values of Nu for variety of nano-fluids when P_r=21. From Table 2 we observe that Nu rises due to rise in G for all nano-fluids, this is true palpably since rise in surface heat flux which accentuates the flow and results in the procurement of enormous heat transfer. It is observed that from Table 2 that Nu rises with rise in suction parameter λ. Nu depreciates with rise of E the reason behind this is that dimensionless surface temperature enhances due to dissipation which enlarges the thermal boundary-layer thickness and Nu shrinks. Nu depreciates with rise in δ. Nu increases with progression of 't' for all nanofluids.

TABLE 2: Numerical values of Nu for a variety of nanofluids when P_r =21

G	λ	E	δ	t	Cu-kerosene	Al_2O_3-kerosene	Ag-kerosene	TiO_2-kerosene	Co-kerosene
5	0.2	0.9	0.04	0.5	0.7874	1.6115	0.3849	1.5404	0.8342
10	0.2	0.9	0.04	0.5	1.0329	1.9526	0.6209	1.8790	1.0723
15	0.2	0.9	0.04	0.5	1.4017	2.3757	1.0009	2.3029	1.4300
5	0.3	0.9	0.04	0.5	1.5362	2.4351	1.0638	2.3534	1.5972
5	0.4	0.9	0.04	0.5	2.4504	3.4071	1.9112	3.3155	2.5264
5	0.2	0.3	0.04	0.5	4.8736	5.0933	4.6562	5.0555	4.9163
5	0.2	0.9	0.02	0.5	1.3979	1.8199	1.1925	1.7843	1.4209
5	0.2	0.9	0	0.5	2.0255	2.0255	2.0255	2.0255	2.0255
5	0.2	0.9	0.04	1	1.4592	2.0756	1.1798	2.0233	1.4859
5	0.2	0.9	0.04	1.5	1.9060	2.3692	1.6741	2.3267	1.9316

Table 3 explains the C_f values respectively for variety of nano-fluids when P_r=21. We noticed that C_f for all nano-fluids grows with rise in G. Physically it is true that elevation in buoyancy, enlarges the shear stress as a result C_f shoots up. As λ escalates the wall shear stress that is C_f diminishes. Elevation in δ reduces the C_f. The C_f progresses with progressing 't'. The C_f increases with growth in E.

TABLE 3: Computational values of C_f for a variety of nanofluids when P_r = 21

G	λ	E	δ	t	Cu-kerosene	Al_2O_3-kerosene	Ag-kerosene	TiO_2-kerosene	Co-kerosene
5	0.2	0.9	0.04	0.5	-0.542	-0.4402	-0.5591	-0.4449	-0.5462
10	0.2	0.9	0.04	0.5	0.0854	0.1583	0.0916	0.1566	0.0761
15	0.2	0.9	0.04	0.5	0.7267	0.7621	0.7595	0.7637	0.7121
5	0.3	0.9	0.04	0.5	-0.6697	-0.5554	-0.6895	-0.5607	-0.6741
5	0.4	0.9	0.04	0.5	-0.8047	-0.6761	-0.828	-0.6821	-0.8093
5	0.2	0.3	0.04	0.5	-0.8336	-0.7154	-0.8599	-0.722	-0.836
5	0.2	0.9	0.02	0.5	-0.437	-0.3861	-0.4456	-0.3884	-0.4391
5	0.2	0.9	0	0.5	-0.3347	-0.3347	-0.3347	-0.3347	-0.3347
5	0.2	0.9	0.04	1	0.0079	0.078	0.005	0.0757	0.0019
5	0.2	0.9	0.04	1.5	0.334	0.3871	0.3417	0.3863	0.3259

CONCLUSIONS

The amplification of heat transfer of Kerosene-nanofluid past a moving porous plate owing to viscous dissipation using Tiwari-Das nanofluid model with Boussinesq approximation is computationally reviewed with the help of Galerkin finite element procedure. The main results are summarized as follows

1. The Kerosene-Alumina nanofluid velocity grows with increasing G E, t and depreciates with increasing λ and δ
2. The Kerosene-Alumina nanofluid temperature intensified with rise in G E, t and deduces with rise in λ and δ.
3. With rise in G, the C_f and the Nu in the vicinity of the surface intensify for all nanofluids.
4. As 't' progressed, the C_f and the Nu in the vicinity of the surface intensify for all nanofluids.
5. The C_f in the vicinity of the surface increased and the Nu depreciates for all nanofluids with the increase in E.
6. With decrease in δ, both the C_f and Nu improve at the surface for all nanofluids.
7. The progression of λ causes a reduction in C_f at the surface and progress of Nu for all nanofluids.
8. Kerosene-Alumina nanofluid attains maximum heat transfer rate and Kerosene-Silver attains minimum rate of heat transfer in contrast with all other nanofluids for all values of G, E, δ, t, λ.This authenticates that utilization of nanofluids plays an indispensible role in amplification of heat transfer rate, and elucidates the prominance of application of nanofluids to rejuvenate the cooling process of engineering and industrial systems.

REFERENCES

1. A.Chen and L.Dang, "Characterization of supercritical JP-7's Heat transfer and coking properties," *40th American Institute of Aeronautics and Astronauts (AIAA) Aerospace sciences Meeting and Exhibit*, AIAA Edited byReno, Reston, Virginia **5,** (2002), pp.1-12.
2. F.Zhong, G.Fan, J.Li.Yu, and C.J.Sung, *Journal of Thermophysics and Heat Transfer* **23,** 543-550 (2009).
3. W. Zhou, Z. Jia, J.Qin, W.Bao and B.Yu, *Chemical Engineering Journal* **243,** 127-136 (2014).
4. Y.X.Hua, Y.Z.Wang and H.Meng, *Journal of Super critical fluids* **52,** 36-46 (2010).
5. Mahmoodi.Mostafa and S.H.Kandelousi, *Propulsion and Power Research* **5,** 279-286 (2016).
6. S.Choi, *American Society of Mechanical Engineers, Fluids Engineering Division* **231,** 99-105 (1995).
7. A.Aziz, and W.A.Khan, *International Journal of Thermal Sciences* **52**, 83-90 (2012).
8. A.V.Kuznetsov and D.A.Nield, *International Journal of Thermal Sciences* 49,243-247 (2010).
9. M.Turkyilmazoglu, *Journal of Heat and Mass Transfer* **136,** 031704-1/031704-7 (2014).
10. V.Rajesh, A.J. Chamkha and M.P.Mallesh, *International Journal of Numerical Methods for Heat and Fluid Flow* **26,** 328-347 (2016).
11. Acharya.Nilankush, Kalidas, Kundu.Prabir Kumar, *Alexandria Engineering Journal* **55,** 1177-1186 (2016).
12. K.Kannaiyan, K.Anoop and R.Sadr, *Journal of Energy Resources Technology-ASME* **139,** 032201-1/032201-8 (2017).
13. F.Shariatmadar and S.Pakdehi, *Energy Fuels* **30,** 7755-7762 (2016).
14. D.Agarwal, A.Vaidyanathan and S.Kumar, *Experimental Thermal and Fluid Science* **71,** 1-43 (2016),
15. P.M. Congedo and S.Collura, *American Society of Mechanical* Engineers*, Summer Heat Transfer Conference, Jackson V*ille, Florida, USA **3,** (2008), pp 1-11.
16. V.Rajesh, A.J. Chamkha. and M.P.Mallesh, *Journal of Applied Fluid Mechanics* **9,** 2457-2467 (2015).
17. P.K.Singh, *International Journal of Engineering Science* **4,** 2647-2656 (2012).

18. N.Kishan and G.Deepa, *Advances in Applied Science Research* **3,** 430-439 (2012).
19. V.Rajesh, M.P.Mallesh and O. Anwar beg, *Procedia Materials Sciences* **10,** 80-89 (2014).
20. M.J.Uddin, M.S.Alam and M.Rahman, *Arabian Journal of Science and Engineering* **42,** 1883-1901. (2017).
21. R.K.Tiwari and M.K.Das , *International Journal of Heat and Mass Transfer* **50,** 2002-2018 (2007).
22. H.Schlichting and K.Gerstein, Boundary layer Theory, *Springer-Verlag*, 8th Edition., New York, USA (2001).
23. J.C.Maxwell Garnett, Philosophical Transactions of the Royal Society of London **203,** 385–420 (1904).
24. H.C.Brinkman, *Journal of Chemical Physics* **24,** 571-581 (1952).
25. V.Rajesh and Ali.J.Chamka *International Journal of Numerical Methods for Heat and Fluid flow* **24,** 1109-1123 **(**2014).
26. J.N.Reddy, *An Introduction to the Finite Element Method*, McGraw-Hill,**3rd** Edition, New York, USA (2006).
27. K.J.Bathe, *Finite Element Procedures,* Prentice-Hall, Upper Saddle River, NJ(1996).
28. B.Carnahan, H.A.Luther and J.O.Wilkes, *Applied numerical methods,* John Wiley and Sons, New York (1969).